

# A PGC-1 $\alpha$ Isoform Induced by Resistance Training Regulates Skeletal Muscle Hypertrophy

Jorge L. Ruas,<sup>1,5,7,\*</sup> James P. White,<sup>1,5</sup> Rajesh R. Rao,<sup>1</sup> Sandra Kleiner,<sup>1,6</sup> Kevin T. Brannan,<sup>1,6</sup> Brooke C. Harrison,<sup>2,6</sup> Nicholas P. Greene,<sup>3</sup> Jun Wu,<sup>1</sup> Jennifer L. Estall,<sup>1</sup> Brian A. Irving,<sup>4</sup> Ian R. Lanza,<sup>4</sup> Kyle A. Rasbach,<sup>1</sup> Mitsuharu Okutsu,<sup>3</sup> K. Sreekumaran Nair,<sup>4</sup> Zhen Yan,<sup>3</sup> Leslie A. Leinwand,<sup>2</sup> and Bruce M. Spiegelman<sup>1,\*</sup>

<sup>1</sup>Department of Cell Biology, Dana-Farber Cancer Institute, Harvard Medical School, Boston, MA 02115, USA

<sup>2</sup>Department of Molecular, Cellular, and Developmental Biology, University of Colorado at Boulder, Boulder, CO 80309, USA

<sup>3</sup>Cardiovascular Medicine, Department of Medicine, University of Virginia, Charlottesville, VA 22908, USA

<sup>4</sup>Endocrine Research Unit, Division of Endocrinology, The Mayo Clinic, 200 1st Street SW, Joseph 5-194, Rochester, MN 55905, USA

<sup>5</sup>These authors contributed equally to this work

<sup>6</sup>These authors contributed equally to this work

<sup>7</sup>Present address: Department of Physiology and Pharmacology, Karolinska Institutet, S-171 77 Stockholm, Sweden

\*Correspondence: jorge.ruas@ki.se (J.L.R.), bruce\_spiegelman@dfci.harvard.edu (B.M.S.)

<http://dx.doi.org/10.1016/j.cell.2012.10.050>

## SUMMARY

PGC-1 $\alpha$  is a transcriptional coactivator induced by exercise that gives muscle many of the best known adaptations to endurance-type exercise but has no effects on muscle strength or hypertrophy. We have identified a form of PGC-1 $\alpha$  (PGC-1 $\alpha$ 4) that results from alternative promoter usage and splicing of the primary transcript. PGC-1 $\alpha$ 4 is highly expressed in exercised muscle but does not regulate most known PGC-1 $\alpha$  targets such as the mitochondrial OXPHOS genes. Rather, it specifically induces IGF1 and represses myostatin, and expression of PGC-1 $\alpha$ 4 in vitro and in vivo induces robust skeletal muscle hypertrophy. Importantly, mice with skeletal muscle-specific transgenic expression of PGC-1 $\alpha$ 4 show increased muscle mass and strength and dramatic resistance to the muscle wasting of cancer cachexia. Expression of PGC-1 $\alpha$ 4 is preferentially induced in mouse and human muscle during resistance exercise. These studies identify a PGC-1 $\alpha$  protein that regulates and coordinates factors involved in skeletal muscle hypertrophy.

## INTRODUCTION

PGC-1 $\alpha$  is a transcriptional coactivator that controls the expression of genes involved in oxidative metabolism. PGC-1 $\alpha$  was originally identified as a coactivator of PPAR $\gamma$  in brown adipose tissue, but it is enriched in many tissues that are active in oxidative metabolism, such as heart, skeletal muscle, and the fasted liver. Muscle PGC-1 $\alpha$  is induced by exercise in both mice and humans (Short et al., 2003). When expressed in skeletal muscle in vivo, PGC-1 $\alpha$  causes many of the changes associated with

endurance training, including mitochondrial biogenesis, fiber-type switching, stimulation of fatty acid oxidation, angiogenesis, and resistance to muscle atrophy (Arany, 2008). This reprogramming of muscle results in increased muscle endurance. Genetic loss of PGC-1 $\alpha$  in murine muscle causes glucose intolerance, especially on a high-fat diet (Choi et al., 2008; Handschin et al., 2007). Elevated PGC-1 $\alpha$  in muscle does not protect against insulin resistance stimulated by a high-fat diet in young mice (Choi et al., 2008) but dramatically protects against the sarcopenia, obesity, and diabetes that accompany aging (Wenz et al., 2009). Although PGC-1 $\alpha$  is induced in exercise and has remarkable effects on muscle endurance, it has no clear-cut effects on either muscle size or strength. Here, we identify a transcript from the *Pgc-1 $\alpha$*  gene that is expressed abundantly in skeletal muscle, particularly in the setting of resistance training in mice and humans. This protein, termed PGC-1 $\alpha$ 4, does not regulate the same set of genes induced by PGC-1 $\alpha$  but rather regulates the IGF1 and myostatin pathways, both of which are known regulators of muscle size and strength (Florini, 1987; McPherron et al., 1997). This results in muscle hypertrophy and increased strength. Remarkably, mice with skeletal-muscle-specific transgenic expression of PGC-1 $\alpha$ 4 show a dramatic resistance to the muscle wasting of cancer cachexia. Taken together, these data suggest that PGC-1 $\alpha$ 4 integrates resistance training with a gene program of muscle hypertrophy, which results in several important health benefits.

## RESULTS

### Identification, Characterization, and Expression of Alternative Isoforms of PGC-1 $\alpha$

We and others have shown that transcription of the *Pgc-1 $\alpha$*  gene can be driven by two distinct promoter regions (Chinsomboon et al., 2009; Yoshioka et al., 2009). One is located immediately 5' of the known exon 1 (proximal promoter), and another (alternative promoter) is located ~13 kb upstream (Figure 1A). By using

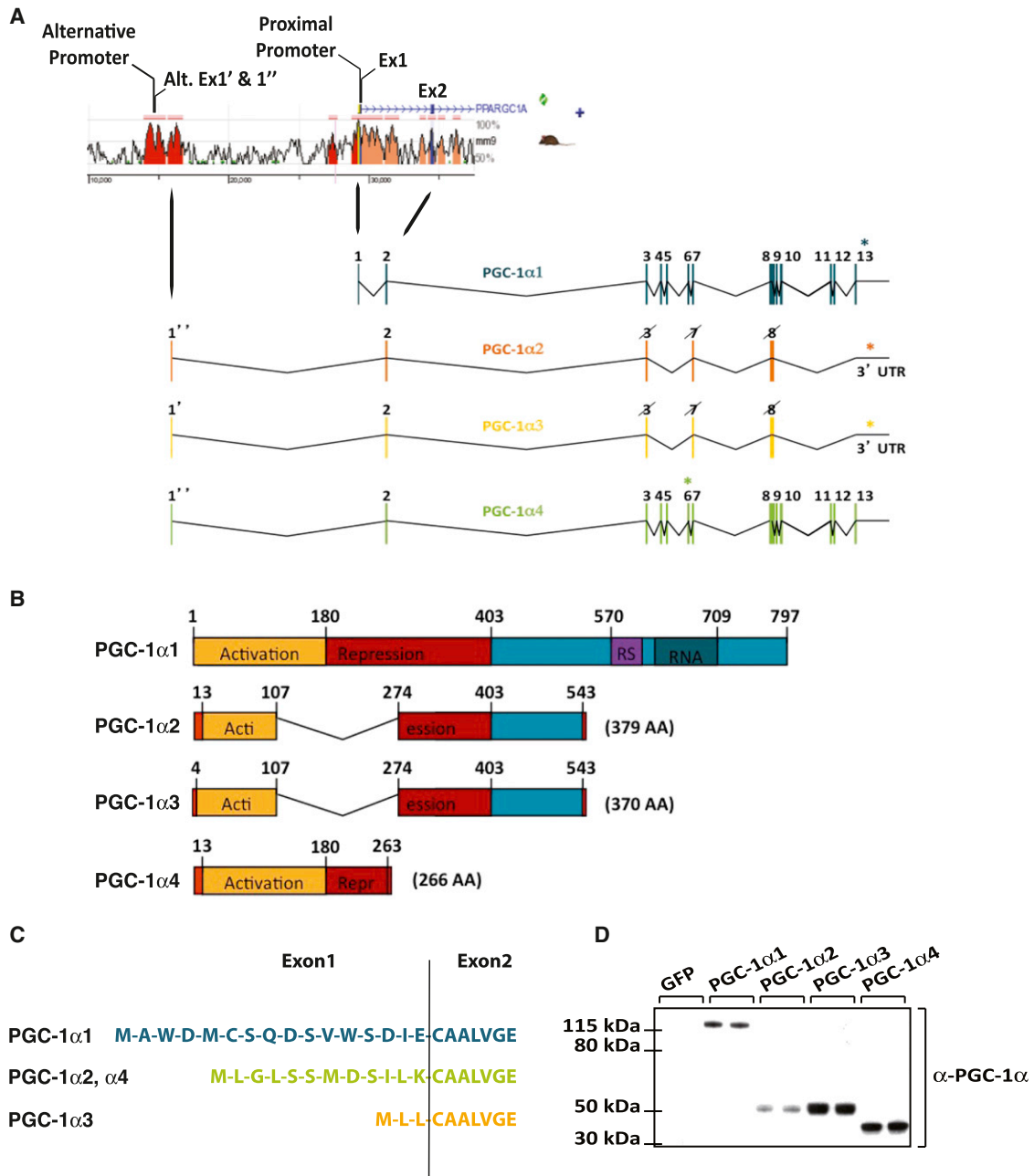


**Figure 1. Cloning and Characterization of PGC-1 $\alpha$  Isoforms**

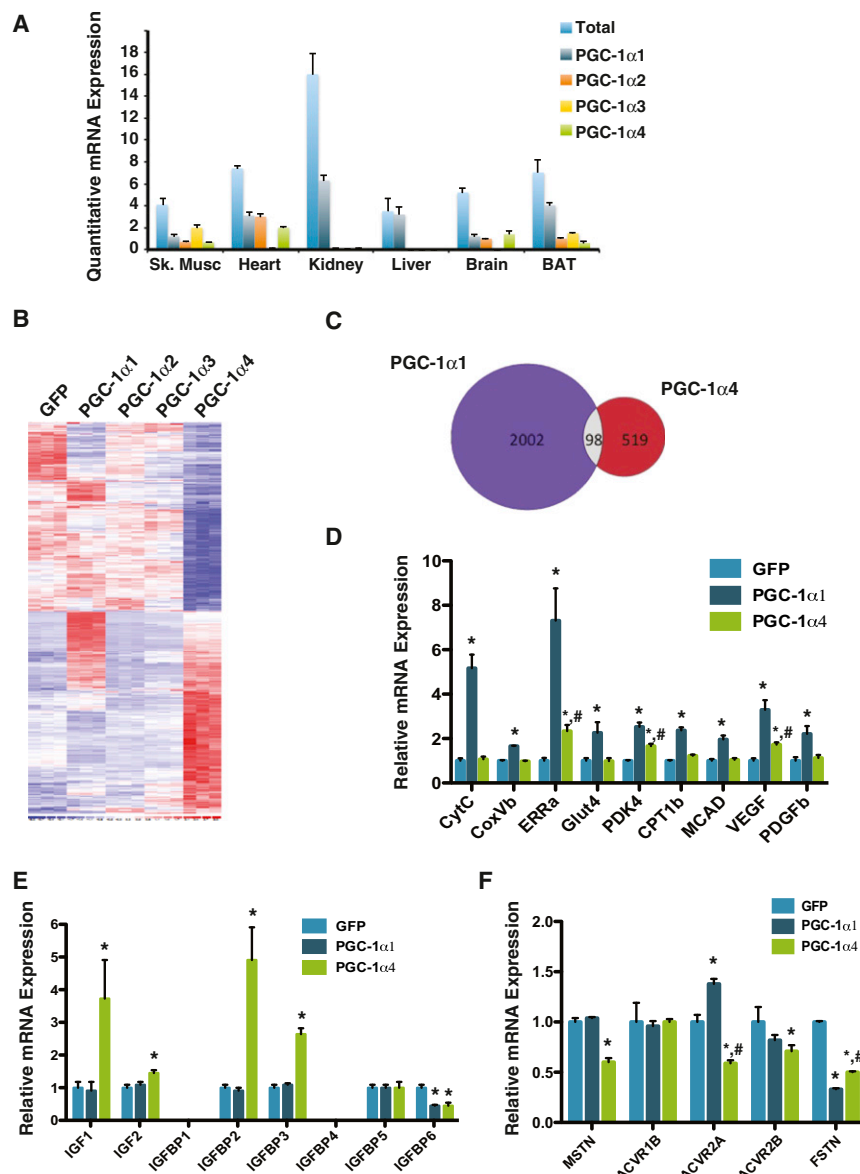
(A) Schematic representation of the conservation between human and mouse PGC-1 $\alpha$  gene (<http://www.dcode.org>). Two promoters that can drive expression of the PGC-1 $\alpha$  gene. Ex indicates exons seen in the depicted region. Structure of the different PGC-1 $\alpha$  isoform mRNA is shown. / indicates partial conservation. \* indicates stop codon.

(B) PGC-1 $\alpha$  protein domain conservation. Amino acid numbers refer to mouse PGC-1 $\alpha$  (hereafter PGC-1 $\alpha$ 1). Numbers in brackets indicate the number of amino acids for each isoform. Red boxes indicate new N- and C-terminal amino acid sequences.

(C) Three different exon1 coding sequences result in different N-terminal amino acid sequences. PGC-1 $\alpha$ 2 and  $\alpha$ 4 share the same alternative exon1 and, therefore, share the same first 12 amino acids. All isoforms share exon 2.

(D) Differential promoter usage and splicing options result in proteins with different molecular weights. The different PGC-1 $\alpha$  isoforms were expressed in HEK293 cells. Whole-cell extracts were resolved by SDS PAGE followed by immunoblotting by using an anti-PGC-1 $\alpha$  antibody (Zhang et al., 2009) that we have found to recognize all isoforms described here.

See also Figure S1.



a targeted PCR strategy (Figure S1A available online), we cloned and characterized the transcripts that result from the use of either promoter in mouse skeletal muscle. We cloned four full-length messenger RNAs (mRNAs); one of these corresponds to the previously described PGC-1 $\alpha$  (hereafter referred to as PGC-1 $\alpha$ 1) and originates exclusively from the proximal promoter. The other three transcripts (hereafter referred to as PGC-1 $\alpha$ 2,  $\alpha$ 3, and  $\alpha$ 4) result from alternative promoter usage and alternative splicing of the *Pgc-1 $\alpha$*  gene (Figures 1A and S1C). The new isoforms encode significantly different proteins (Figure 1B). PGC-1 $\alpha$ 2 and  $\alpha$ 3 have distinct first exons but have the same remaining exon/intron structure (Figure S1C); this results in two new proteins with overall similar domain structure but discrete N termini (Figure 1C). PGC-1 $\alpha$ 2 and  $\alpha$ 3 are 379 and 370 amino acids long and have a predicted molecular weight of

## Figure 2. Gene Expression Profiling of PGC-1 $\alpha$ Isoforms and Their Target Genes

(A) Tissue-specific PGC-1 $\alpha$  isoform expression patterns. Absolute quantification of gene expression in mouse tissues ( $n = 6$ ) by quantitative real-time PCR using isoform-specific primers.

(B) Heatmap summary of relative changes in gene expression by each PGC-1 $\alpha$  isoform. Gene expression was analyzed (Affymetrix) in myotubes expressing GFP alone (control) or together with each PGC-1 $\alpha$  isoform. Experiments were performed in triplicate, and results were analyzed with dChip software.

(C) Venn diagram represents the number of genes regulated by PGC-1 $\alpha$ 1, PGC-1 $\alpha$ 4, and in common between both isoforms.

(D–F) From the Affymetrix results, gene sets were validated by quantitative real-time PCR using specific primers. RNA was prepared as described in (B). Bars depict mean values, and error bars represent SD. \* $p < 0.05$  between indicated group and control. # $p < 0.05$  between all groups. See also Figure S2.

41.9 and 41.0 kDa, respectively. PGC-1 $\alpha$ 4 shares the same alternative exon1 with PGC-1 $\alpha$ 2 (and therefore the same N terminus, Figure 1C), but its mRNA structure is different in that it contains a 31 nucleotide insertion between exons 6 and 7, which generates a premature stop codon (Figures 1A, 1B, and S1C). PGC1 $\alpha$ 4 is predicted to encode 266 amino acids, a protein of 29.1 kDa. The different alternative first exons generate different N termini that seem to significantly affect protein accumulation (Figures 1C, 1D, and S1B). With the use of specific qPCR probes, we determined total PGC-1 $\alpha$  mRNA content (targeting exon 2, which is present in all forms) or the expression of each individual isoform in an array of mouse tissues (Figure 2A).

In fed liver, PGC-1 $\alpha$ 1 levels approach total PGC-1 $\alpha$  content, and no significant alternative isoform expression is observed (Figure 2A). However, in skeletal muscle, heart, and brown adipose tissue (BAT), all isoforms are expressed at comparable levels and represent a significant part of total PGC-1 $\alpha$  mRNA. Figures S2A and S2B show PGC-1 $\alpha$  isoform protein levels in superficial white quadriceps (glycolytic, low PGC-1 $\alpha$ 1 levels) and tibialis anterior (oxidative, high PGC-1 $\alpha$ 1 levels) muscle, as well as liver, kidney, and BAT. Primary myotubes treated with the known PGC-1 $\alpha$  inducer forskolin show high levels of all isoforms (Figure S2C). Similarly, cold exposure induces expression of all PGC-1 $\alpha$  variants in BAT (Figures S2D and S2E). These results show that total PGC-1 $\alpha$  mRNA content includes significant levels of each isoform, which can be increased in vitro and in vivo by known inducers of the *Pgc-1 $\alpha$*  gene.

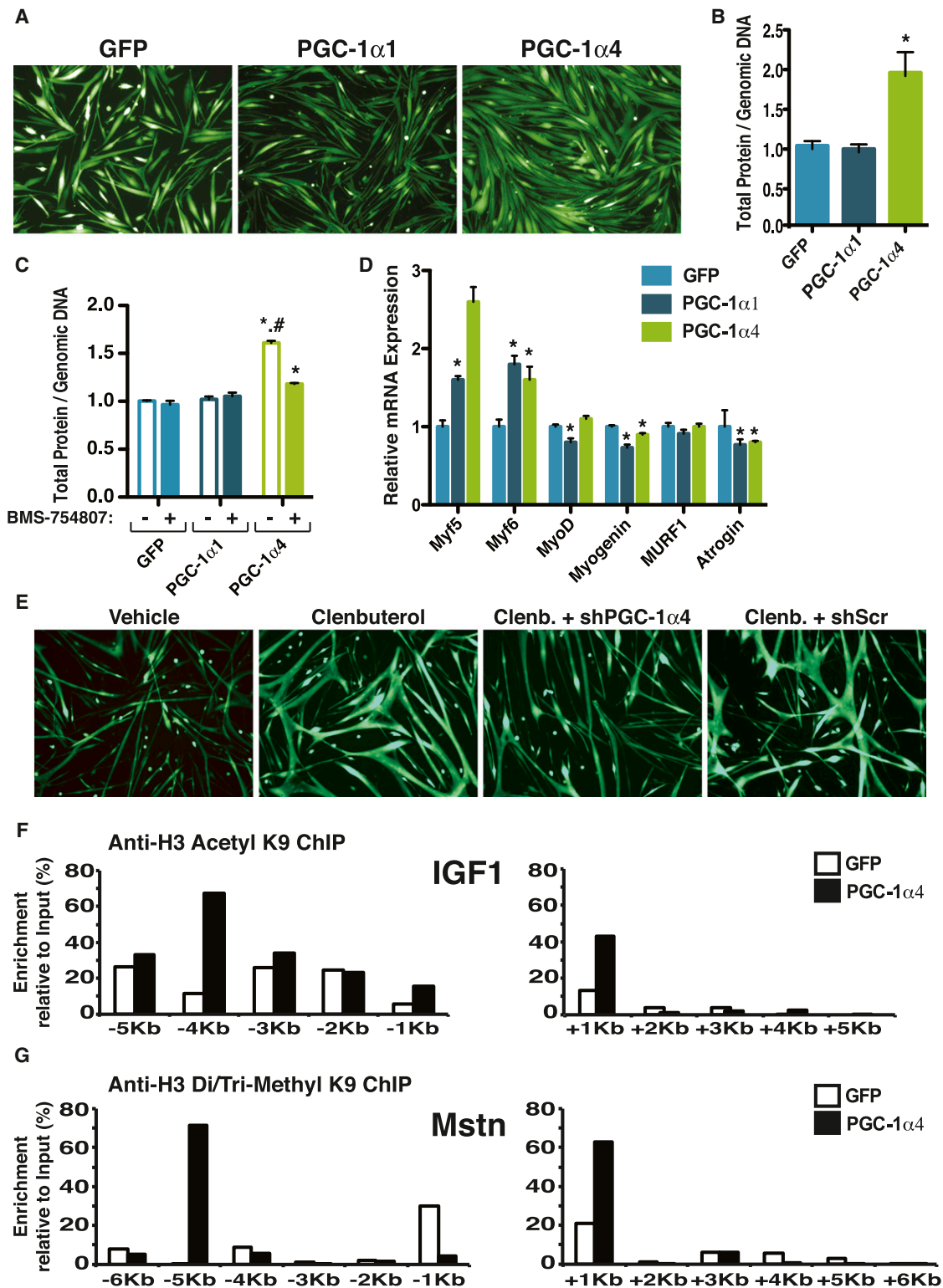


**Figure 3. Myotubes Expressing PGC-1 $\alpha$ 4 Show Cellular Hypertrophy**

(A) Fluorescence microscopy analysis of myotubes expressing GFP alone or together with PGC-1 $\alpha$ 1 or PGC-1 $\alpha$ 4. Fully differentiated myotubes were transduced with the different adenovirus and were observed under a fluorescence microscope 36 hr later with a 10 $\times$  objective.

(B) Protein accumulation normalized by genomic DNA content in myotubes expressing GFP control, PGC-1 $\alpha$ 1, or PGC-1 $\alpha$ 4. Experiments were performed as described in (A), but cells were processed for either total protein or DNA quantification. Graphs show the total protein/genomic DNA ratio.

### PGC-1 $\alpha$ 4 Regulates a Discrete Gene Program in Primary Myotubes

Differentiated primary myotubes were transduced with adenovirus expressing different PGC1 $\alpha$  isoforms. Figure 2B shows a heat map generated by comparing the gene expression profile of cells receiving each PGC-1 $\alpha$  isoform, compared to green fluorescent protein (GFP) alone. Interestingly, PGC-1 $\alpha$ 1 and PGC-1 $\alpha$ 4 drive many changes in gene expression that are distinct from each other; only 98 genes were coregulated by both PGC-1 $\alpha$ 1 and PGC-1 $\alpha$ 4 (Figure 2C). PGC-1 $\alpha$ 2 and 3 seem to affect the expression of only a very small set of genes (110 and 69 gene IDs, respectively). The functions of PGC-1 $\alpha$ 2 and  $\alpha$ 3 remain under investigation. Importantly, expression of PGC-1 $\alpha$ 4 in myotubes did not affect the regulation of many classic PGC-1 $\alpha$ 1 targets, including CytC (cytochrome C), CoxVb (cytochrome c oxidase subunit Vb), Glut4 (glucose transporter type 4), CPT1 (carnitine palmitoyltransferase-I), MCAD (medium chain acyl CoA dehydrogenase), and PDGFb (platelet-derived growth factor B) (Figure 2D). Several other known PGC-1 $\alpha$  target genes were induced by PGC-1 $\alpha$ 4 expression, though to a much lesser extent than upon expression of PGC-1 $\alpha$ 1 (Figure 2D), including ERR $\alpha$ , PDK4 (pyruvate dehydrogenase kinase, iso-enzyme 4), and VEGFa (vascular endothelial growth factor A). These results strongly suggest distinct functions for PGC-1 $\alpha$ 1 and PGC1 $\alpha$ 4.

### Expression of PGC-1 $\alpha$ 4 Specifically Induces IGF1 and Represses Myostatin Gene Expression

Pathway analysis of the microarray data identified cell morphology, growth, and proliferation and IGF1 signaling as the top pathways predicted to be under PGC-1 $\alpha$ 4 regulation (data not shown). From quantitative real-time PCR, we confirmed that PGC-1 $\alpha$ 4 (but not  $\alpha$ 1) specifically induces expression of IGF1 (3.7-fold) while minimally affecting IGF2 (1.5-fold) levels (Figure 2E). The expression levels of some members of the IGF-binding protein (IGFBP) family were also selectively affected by PGC-1 $\alpha$ 4 expression. IGF1 is among the best-known activators of skeletal muscle hypertrophy (Adams, 2002). PGC-1 $\alpha$ 4 expression also reduced mRNA levels of myostatin, a powerful, negative regulator of muscle size in rodents and humans (Figure 2F) (Lee, 2004; McPherron et al., 1997), as well as the transcript levels of its receptors ACVR1a and ACVR1b (40% and 30%, respectively). The levels of ACVR1b remained unaffected by expression of either PGC-1 $\alpha$ 1 or PGC1 $\alpha$ 4, whereas both iso-

forms repress follistatin expression (Figure 2F). Taken together, these results indicate that PGC-1 $\alpha$ 4 controls the expression of genes in two important pathways for regulating skeletal muscle size.

### PGC-1 $\alpha$ 4 Expression Leads to Powerful Myotube Hypertrophy

Myotubes expressing PGC-1 $\alpha$ 4 appear significantly larger than those expressing GFP control or PGC-1 $\alpha$ 1 (Figure 3A), with a 2-fold elevation in the ratio of total protein to genomic DNA (Figure 3B). We observed no significant differences in fusion of myoblasts expressing GFP or the different PGC-1 $\alpha$  isoforms, as assessed by the number of nuclei per myotube (Figure S3A). Importantly, the PGC-1 $\alpha$ 4-dependent increase in myotube size and protein accumulation could be inhibited by an IGF1 receptor (IGF1R) inhibitor (BMS-754807; Dinchuk et al., 2010) (Figures 3C and S3B). Under the same conditions, no significant changes in total protein accumulation were observed in cells expressing GFP or PGC-1 $\alpha$ 1. Although we observed an increase in expression of the myogenic transcription factors Myf5 and 6, the levels of MyoD and myogenin were only minimally affected (Figure 3D). Small effects were also observed in the expression of the atrophy-related genes MuRF-1 and atrogin-1/MAFbx (Figure 3D) (Bodine et al., 2001; Gomes et al., 2001). Both PGC-1 $\alpha$  isoforms show a predominantly nuclear localization in skeletal myotubes (Figure S3C). Taken together, these results clearly suggest a role for PGC-1 $\alpha$ 4 in the regulation of myotube size and protein content, mediated (at least in part) by IGF1.

### PGC-1 $\alpha$ 4 Loss of Function Blunts Skeletal Muscle Cell Hypertrophy in Culture

To evaluate the requirement for PGC-1 $\alpha$ 4 in a cellular model of skeletal muscle hypertrophy, we developed an isoform-specific short hairpin RNA (shRNA). As shown in Figure S3D, PGC-1 $\alpha$ 4 shRNA efficiently reduces PGC-1 $\alpha$ 4 mRNA levels in transduced myotubes while not affecting PGC-1 $\alpha$ 1. Myotube hypertrophy was induced by treatment with the  $\beta$ -adrenergic agonist clenbuterol (McMillan et al., 1992); this resulted in robust hypertrophy (Figure 3E) accompanied by a 5-fold increase in endogenous PGC-1 $\alpha$ 4 levels and also resulted in a 1.9-fold increase in protein/DNA ratio (Figures S3D and 3E). No changes were observed in PGC-1 $\alpha$ 1 levels with clenbuterol treatment. However, shRNA-mediated reduction in PGC-1 $\alpha$ 4 levels blunted clenbuterol-induced myotube hypertrophy (Figure 3E) and protein

(C) Protein accumulation normalized by genomic DNA content in myotubes expressing GFP control, PGC-1 $\alpha$ 1, or PGC-1 $\alpha$ 4 and treated with the IGF1R inhibitor BMS-754807. Myotubes were transduced as described in (A) and treated with 5 nM BMS-754807. At the end of 36 hr, cells were processed for total protein or DNA quantification.

(D) Analysis of gene expression for markers of myogenic differentiation. Experiments were performed as described in (A), and gene expression was analyzed by quantitative real-time PCR by using primers specific to the indicated genes.

(E) PGC-1 $\alpha$ 4 loss of function blunts clenbuterol-induced myotube hypertrophy. Fully differentiated primary myotubes were treated with 500 nM Clenbuterol (or vehicle) and transduced with adenovirus expressing PGC-1 $\alpha$ 4-specific or scrambled control shRNAs. 48 hr later, cells were processed for fluorescence microscopy or analysis of protein/DNA content.

(F) ChIP of DNA regions associated with Acetyl-H3K9. Myotubes expressing GFP alone or with PGC-1 $\alpha$ 4 were processed for ChIP. Purified DNA fragments were identified and quantified by PCR using primers targeting the IGF1 gene at 1 kb intervals. Graph shows enrichment relative to input after normalized by IgG.

(G) ChIP of regions associated with di/trimethyl-H3K9. Myotubes were processed as described above. Purified DNA fragments were identified and quantified by PCR using primers targeting the Myostatin gene at 1 kb intervals. Graph shows enrichment relative to input normalized by IgG.

Bars depict mean values, and error bars represent SD. \* $p < 0.05$  between indicated group and control. # $p < 0.05$  between all groups. See also Figure S3.

accumulation, compared to a scrambled control (Figure S3E). These results show that PGC-1 $\alpha$ 4 is required for myotube hypertrophy in this cellular model.

#### Loss of Estrogen-Related Receptors $\alpha$ or $\gamma$ Does Not Affect PGC-1 $\alpha$ 4-Mediated Myotube Hypertrophy

The estrogen-related receptors are master drivers of OXPHOS gene expression under PGC-1 $\alpha$ 1 coactivation (Giguère, 2008). We investigated whether myotubes genetically deficient in ERR $\alpha$  or ERR $\gamma$  could still support PGC-1 $\alpha$ 4 function. Differentiated myotubes were transduced with adenovirus expressing GFP control or PGC-1 $\alpha$ 4, and even in the absence of ERR $\alpha$ , PGC-1 $\alpha$ 4 was still able to induce robust myotube hypertrophy (Figure S4F); both IGF1 and myostatin genes were regulated as previously observed in wild-type cells (Figure S3G). Similar results were obtained with ERR $\gamma$ -deficient myotubes (data not shown). In agreement with these results, and in contrast to PGC-1 $\alpha$ 1, PGC-1 $\alpha$ 4 did not coactivate ERR $\alpha$  function in luciferase assays using two different reporters for ERR-mediated transactivation (Figure S3H). These results indicate that PGC-1 $\alpha$ 4 does not coactivate ERR function, which likely contributes to the lack of effect on OXPHOS gene expression.

#### PGC-1 $\alpha$ 4 Expression Induces Changes in Histone Modifications near the IGF1 and Myostatin Genes

The PGC-1s have been shown to associate with other coregulatory complexes to promote chromatin remodeling and enhance transcription of target genes. One such complex is anchored by the histone acetyltransferase CBP/p300, which mediates histone tail acetylation as a mark for positive gene regulation (Ogryzko et al., 1996). Because IGF1 gene transcription is enhanced by PGC-1 $\alpha$ 4, we performed chromatin immunoprecipitation (ChIP) experiments by using an anti-acetyl-H3K9 antibody to identify potential IGF1 gene enhancer regions. We thus identified three regions of DNA where association with acetyl-H3K9 was significantly enriched upon expression of PGC-1 $\alpha$ 4 (Figure 3F). Those included the gene promoter (2.7-fold) and 3' untranslated region (UTR) (3.3-fold) and a region located 4 kb upstream of the transcription initiation site (5.9-fold). To identify regions of the myostatin gene that could mediate the repressive effect of PGC-1 $\alpha$ 4, we performed ChIP experiments targeting DNA regions associated with di/trimethyl-H3K9, a mark for negative gene regulation (Heard et al., 2001). Of the identified regions, a sequence located 5 kb upstream of the myostatin gene showed the highest PGC-1 $\alpha$ 4-induced association with di/trimethyl-H3K9 (74.3-fold) (Figure 3G), suggesting the potential location of a regulatory region. Upon expression of PGC-1 $\alpha$ 4, the 3' UTR of the myostatin gene showed a 3.2-fold higher association with di/tri-methyl-H3K9, whereas the gene promoter showed a decrease of 80%. These results identify putative regulatory regions near the IGF1 and myostatin genes, which could be the target of PGC-1 $\alpha$ 4-mediated regulation.

#### Delivery of PGC-1 $\alpha$ 4 to Skeletal Muscle Causes Marked Hypertrophy *In Vivo*

To evaluate the effect of PGC-1 $\alpha$ 4 expression *in vivo*, we performed intramuscular injections of the adenoviral vectors. Mice

with severe combined immunodeficiency (SCID) were used to maximize adenovirus uptake by muscle and to reduce any immune response to the adenoviruses (Chakkalakal et al., 2010). Each mouse received an injection of GFP control adenovirus into the gastrocnemius of one limb (Figure S4A) and received an equivalent injection of a PGC-1 $\alpha$ 4-expressing adenovirus into the contralateral limb. Fibers expressing PGC-1 $\alpha$ 4 showed a 59.5% increase in average cross-sectional area (CSA) 7 days after injection, compared to controls (Figures 4A and S4B). In particular, PGC-1 $\alpha$ 4 drove the appearance of very large fibers (in the >1,200  $\mu\text{m}^2$  interval) that were rarely seen with the control (Figure 4B). PGC-1 $\alpha$ 4 expression *in vivo* resulted in a 2.3-fold increase in IGF1 gene expression and in a 50% reduction in myostatin gene expression (Figure S4C). Furthermore, PGC-1 $\alpha$ 4 expression in muscle resulted in increased S6 ribosomal protein phosphorylation levels (Figure S4D), which is indicative of S6K activation (Pende et al., 2004).

We also performed electroporation of plasmids encoding PGC-1 $\alpha$ 4 (or a control) into the tibialis anterior of C57Bl/6 mice. As before, each mouse received the control plasmid in one limb and received the PGC-1 $\alpha$ 4-expression plasmid in the contralateral limb. Recently, another PGC-1 $\alpha$  splicing variant has cloned from a mouse BAT complementary DNA (cDNA) library and was named NT-PGC-1 $\alpha$  (Zhang et al., 2009). Although we have been unable to detect expression of endogenous NT-PGC-1 $\alpha$  transcript in skeletal muscle, we tested whether electroporation of a plasmid encoding this PGC-1 $\alpha$  variant would induce changes in the CSA of targeted fibers, as observed for PGC-1 $\alpha$ 4. Although PGC-1 $\alpha$ 4 and NT-PGC-1 $\alpha$  mRNAs were expressed at similar levels (Figure 4C), we could not detect NT-PGC-1 $\alpha$  protein accumulation by immunoblotting (Figure 4D). We observed an average increase of 28% in CSA of PGC-1 $\alpha$ 4-expressing fibers when compared to controls (Figure S4E). Results are also shown as CSA frequency distribution in Figure 4E and show a 34.7% reduction in the smallest CSA interval (<1,000  $\mu\text{m}^2$ ) and show increases of 45.5% and 99.4% in the -2,000 and -2,500  $\mu\text{m}^2$  intervals (respectively). As before, we observed fibers of CSA in the -3,000 and >3,000  $\mu\text{m}^2$  intervals, which were not significantly observed in controls (Figure 4E). This increase in average CSA was accompanied by a 10% increase in muscle weight, compared to control limb (Figure S4F). PGC-1 $\alpha$ 4 expression resulted in higher phospho-S6K levels (Figure S4G). Expression of NT-PGC-1 $\alpha$  resulted in a decrease of 46.7% and 66.9% in the number of larger fibers with CSA in the -2,000 and -2,500  $\mu\text{m}^2$  intervals (respectively) and resulted in an increase of 33.8% in smaller fibers with CSA in the -1,500  $\mu\text{m}^2$  interval (Figure 4F). These results indicate that *in vivo* delivery of PGC-1 $\alpha$ 4 results in a marked increase in the CSA of targeted fibers.

#### Regulation of PGC-1 $\alpha$ 4 Expression during Hindlimb Suspension/Reloading

We next investigated whether PGC-1 $\alpha$ 4 levels are regulated by a hindlimb suspension/reloading protocol, a model of skeletal muscle hypertrophy in rodents (Hanson et al., 2010). As shown in Figure 5A, hindlimb suspension resulted in a small but significant decrease in total PGC-1 $\alpha$  content in the soleus muscle (0.85-fold when compared to control), and reloading resulted

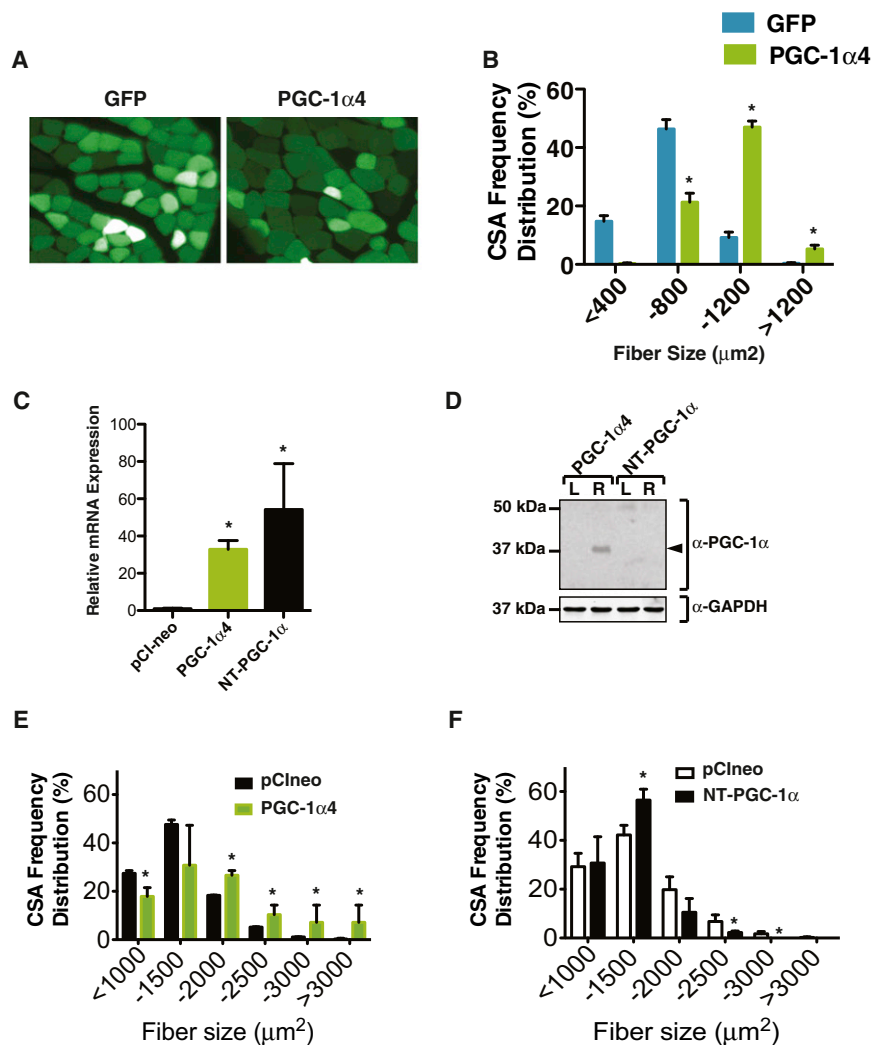


#### Figure 4. In Vivo Expression of PGC-1 $\alpha$ 4 Induces Skeletal Muscle Hypertrophy

(A) Adenovirus-mediated expression of PGC-1 $\alpha$ 4 in mouse skeletal muscle. Cross-section of the gastrocnemius muscle 7 days after intramuscular injection of adenovirus expressing GFP alone or with PGC-1 $\alpha$ 4.

(B) Cross-sectional area frequency distribution (sections from six mice per group).

(C) PGC-1 $\alpha$ 4 and NT-PGC-1 $\alpha$  mRNA expression levels in electroporated tibialis anterior analyzed by quantitative real-time PCR using primers targeting exon 2 (present in both isoforms).

(D) PGC-1 $\alpha$ 4 and NT-PGC-1 $\alpha$  protein expression levels in electroporated muscle.

(E and F) Electroporation-mediated delivery of plasmids into the tibialis anterior (TA). Each mouse ( $n = 6$  per group) received a control plasmid in one limb (pCI-neo) and received in the contralateral limb the plasmid encoding PGC-1 $\alpha$ 4 or NT-PGC-1 $\alpha$ . Bars depict mean values, and error bars represent SE. \* $p < 0.05$  between indicated group and control.

See also Figure S4.

#### Different Exercise Protocols Result in Differential PGC-1 $\alpha$ Isoform Expression in Human Muscle

We determined the expression of PGC-1 $\alpha$ 4 in human skeletal muscle with training. Percutaneous muscle biopsies of the vastus lateralis muscle were obtained at baseline and 48 hr after the last training session. Figure 5C shows the change in total PGC-1 $\alpha$  expression at the end of the indicated exercise protocol (Table S1). All exercise programs elevated total PGC-1 $\alpha$  levels in muscle, although to different degrees. Notably,

in a 1.6-fold increase. Changes in muscle wet weights are shown in Figure S5A. No significant changes in PGC-1 $\alpha$ 1 mRNA levels were observed upon suspension, but a marked reduction was seen after reloading (50% versus control), when hypertrophic signaling cascades are initiated. Accordingly, during the suspension and reloading phases, we observed a reduction in the expression of transcripts driven by the proximal promoter of the PGC-1 $\alpha$  gene, as assessed by quantitative real-time PCR using primers directed at that 5' UTR region (Figure S5B). Interestingly, PGC-1 $\alpha$ 4 expression levels drop to 22% of starting levels after suspension and increase by 18.7-fold with reloading (Figure 5A). The increase in PGC-1 $\alpha$ 4 mRNA expression during the reloading phase was accompanied by significant protein accumulation (Figure S5C). This expression pattern matches the suspension/atrophy and reloading/hypertrophy phases and coincided with an increase in IGF1 and a decrease in myostatin gene expression (1.8-fold and 40%, respectively; Figure 5B). Similar results were obtained with the gastrocnemius/plantaris muscles (Figures S5A and S5D).

the combined endurance/resistance protocol induced the most significant increase in PGC-1 $\alpha$  expression. We observed no changes in PGC-1 $\alpha$ 4 expression in the endurance protocol group (Figure 5D). However, both the resistance and the combined exercise programs led to a 1.5- and 3-fold increase in the expression of PGC-1 $\alpha$ 4 (respectively). We observed a reduction in myostatin gene expression only in the resistance and combined groups (Figure 5E) but observed no statistically significant changes in IGF1 expression (Figure 5F). Interestingly, a very significant correlation across all groups ( $R = 0.64$ ) was observed between the changes in PGC-1 $\alpha$ 4 expression and performance in the leg press exercise (Figure 5G).

#### Transgenic Muscle-Specific Expression of PGC-1 $\alpha$ 4 Drives Increased Muscle Mass, Strength, and Reduced Adiposity

To evaluate the effects of chronically elevated PGC-1 $\alpha$ 4 levels in muscle, we generated the transgenic mouse model Myo-PGC-1 $\alpha$ 4. This mouse (Figure 5H) expresses PGC-1 $\alpha$ 4 under the control of a MEF2C enhancer/myogenin promoter (Li et al.,

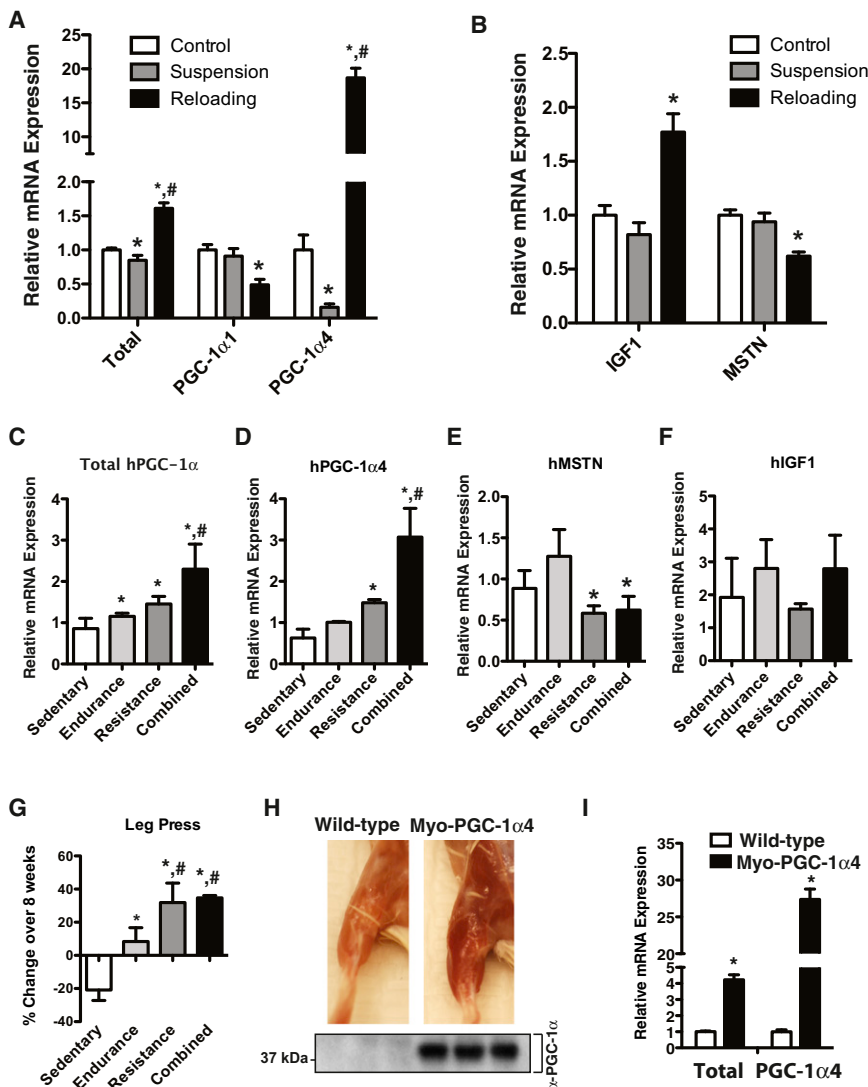


**Figure 5. PGC-1 $\alpha$ 4 Expression Increases during Muscle Hypertrophy and Resistance Training**

(A and B) PGC-1 $\alpha$ 4 expression increases during the hypertrophy phase of a suspension/reloading protocol. C57Bl/6 mice were divided into groups (n = 4 each): control, 10 days hindlimb suspension (Suspension) or 10 days suspension plus 24 hr of reloading (Reloading). The soleus muscles were harvested and processed for gene expression analysis by quantitative real-time PCR using primers specific for the indicated genes.

(C–F) Analysis of gene expression in skeletal muscle biopsies from human volunteers. Percutaneous vastus lateralis biopsies were obtained at baseline and 8 weeks later, ~48 hr after the last training session. Gene expression was analyzed by quantitative real-time PCR using primers specific to the indicated genes.

(G) Increase in PGC-1 $\alpha$ 4 expression correlates with improvement in leg press exercise performance. Graph shows the percent change in the number of leg press repetitions observed between baseline and after 8 weeks of training.

(H) Morphology of hindlimbs from wild-type and PGC-1 $\alpha$ 4 transgenic mice (Myo-PGC1 $\alpha$ 4). Immunoblot using an anti-PGC-1 $\alpha$  antibody ( $\alpha$ -PGC-1 $\alpha$ ) shows PGC-1 $\alpha$ 4 protein levels in the gastrocnemius muscle.

(I) Total PGC-1 $\alpha$  and PGC-1 $\alpha$ 4 mRNA levels in the Myo-PGC-1 $\alpha$ 4 mouse line were determined by quantitative real-time PCR and compared to the wild-type littermate controls. Bars depict mean values, and error bars represent SD. \*p < 0.05 between indicated group and control. #p < 0.05 between all groups. See also Figure S5.

2005). Transgenic muscle expresses PGC-1 $\alpha$ 4 mRNA 30-fold above endogenous levels (Figure 5I) and shows significant PGC-1 $\alpha$ 4 protein accumulation (Figure 5H). Importantly, these levels of expression bring PGC-1 $\alpha$ 4 levels up to those observed during the reloading phase of the suspension/reloading experiments (i.e., 19-fold, Figure 5A). Analysis of the Myo-PGC-1 $\alpha$ 4 mouse shows redder muscle when compared to the wild-type littermate controls (Figure 5H). The pattern of gene expression observed in the muscle of Myo-PGC-1 $\alpha$ 4 mice (Figure S5E) was similar to the one observed upon expression of PGC-1 $\alpha$ 4 in myotubes (Figures 2D–2F) with the exception of IGF1. In these animals, and consistent with our previous results, we observed a 64.4% reduction in myostatin expression. However, there was no increase in IGF1 expression (Figure S5E). PGC-1 $\alpha$ 4 transgenic mice showed an increase in muscle wet weight as observed in Figure 6A. The increase in muscle mass was accompanied by an average increase of 12% in fiber CSA (Figure 6B), with a significant increase in larger fibers (Figures S6A and

also show reduced adiposity. Skeletal-muscle-specific PGC-1 $\alpha$ 4 transgenics show a reduction of 20.7% and 40% in the mass of the epididymal and retroperitoneal fat depots (Figure 6D). Among the tissues analyzed, this observation proved to be selective to fat (Figure S6D). When compared to the wild-type controls, the PGC1 $\alpha$ 4 transgenics show a 20% increase in maximum force generated (Figure 6E). Interestingly, transgenic muscle also proved to be more fatigue-resistant than wild-type (Figure 6F). These results show that elevation of PGC-1 $\alpha$ 4 levels in skeletal muscle results in a hypertrophy phenotype accompanied by a significant increase in strength.

**Myo-PGC-1 $\alpha$ 4 Mice Show Less Muscle Loss upon Hindlimb Suspension and Improved Exercise Performance**

To evaluate the physiological alterations in the Myo-PGC-1 $\alpha$ 4 mouse, we performed hindlimb suspension/reloading experiments. Myo-PGC-1 $\alpha$ 4 mice lost significantly less muscle mass

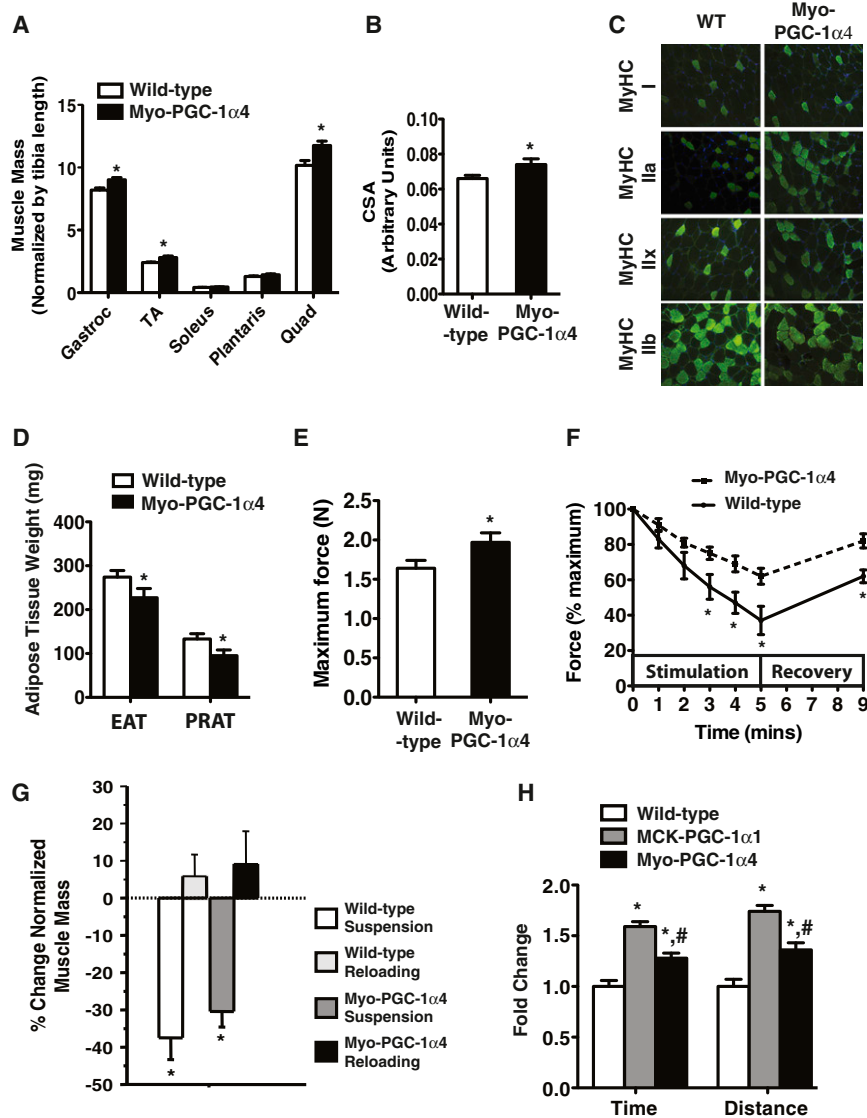


**Figure 6. Myo-PGC-1 $\alpha$ 4 Skeletal Muscle Transgenics Have Increased Muscle Mass and Strength**

(A) Determination of muscle wet weight from PGC-1 $\alpha$ 4 transgenics and wild-type controls (n = 6). Muscle weights are normalized by tibia length.

(B) Fiber cross-sectional area in the gastrocnemius muscle of wild-type and PGC-1 $\alpha$ 4 transgenics.

(C) Immunohistochemical analysis of gastrocnemius muscle from wild-type (WT) and Myo-PGC-1 $\alpha$ 4 animals by using antibodies against different myosin heavy chain (MyHC) types.

(D) Determination of Epididimal (EAT) and Perirenal (PRAT) adipose tissue wet weight from PGC-1 $\alpha$ 4 transgenics and wild-type controls (n = 6).

(E) Maximal force measurements of the gastrocnemius muscle of wild-type and PGC-1 $\alpha$ 4 transgenics (Myo-PGC-1 $\alpha$ 4).

(F) Muscle fatigue test performed under the same experimental settings as in (E).

(G) Changes in normalized muscle mass with hindlimb suspension/reloading. n = 4 per group.

(H) Exercise tolerance test. Muscle-specific PGC-1 $\alpha$ 1 (MCK-PGC-1 $\alpha$ ) and PGC-1 $\alpha$ 4 (Myo-PGC-1 $\alpha$ 4) transgenics ran to exhaustion on a treadmill. Data are normalized by values obtained with wild-type animals (n = 6 per group). Bars depict mean values, and error bars represent SE. \*p < 0.05 between indicated group and control. #p < 0.05 between all groups.

See also Figure S6 and Table S1.

during the suspension phase (Figure 6G) and trended toward accumulating more muscle mass during the reloading process. Myo-PGC-1 $\alpha$ 4 mice were evaluated for their performance on an exercise tolerance test and were compared to littermate controls and to the previously reported mice with muscle-specific PGC-1 $\alpha$ 1 expression (MCK-PGC-1 $\alpha$ ). As expected (Lin et al., 2002), MCK-PGC-1 $\alpha$  mice remained on the treadmill 60% longer than controls (Figure 6H). The Myo-PGC-1 $\alpha$ 4 mice showed improved performance, with a 28% increase in time to exhaustion compared to controls (Figure 6H). No differences in glucose tolerance were observed between these mouse models and controls (Figure S6E). Metabolic profiling of the Myo-PGC-1 $\alpha$ 4 mice by using Comprehensive Laboratory Animal Monitoring System (CLAMS) revealed that, although these animals have higher maximum oxygen consumption (VO<sub>2</sub>) and carbon dioxide elimination (VCO<sub>2</sub>), their respiratory exchange ratio (RER) is unchanged (Figure S6F). No changes

in food consumption (Figure S6F) or movement (data not shown) were observed. These results show that the increase in muscle mass and strength observed in the Myo-PGC-1 $\alpha$ 4 mice does not result in an overt metabolic phenotype but contributes to better exercise performance and protects against hindlimb unloading-induced atrophy.

#### Myo-PGC-1 $\alpha$ 4 Mice Show Resistance to Cancer-Induced Cachexia with Improved Glucose Tolerance and Preserved Muscle Mass

Cancer cachexia is a very important complication of many malignancies, resulting in severe muscle wasting and negatively affecting patient outcome (Fearon et al., 2012). Wild-type and Myo-PGC-1 $\alpha$ 4 mice were inoculated with the Lewis lung carcinoma (LLC) cells, and the cachectic phenotype was evaluated 24–28 days after inoculation. Importantly, this model of cachexia is characterized by loss of muscle mass and strength and by development of glucose intolerance (Busquets et al., 2012; Das et al., 2011). Upon necropsy analysis of tumor-bearing animals, muscles of Myo-PGC-1 $\alpha$ 4 mice looked less pale and healthier when compared to cachectic muscle from wild-type

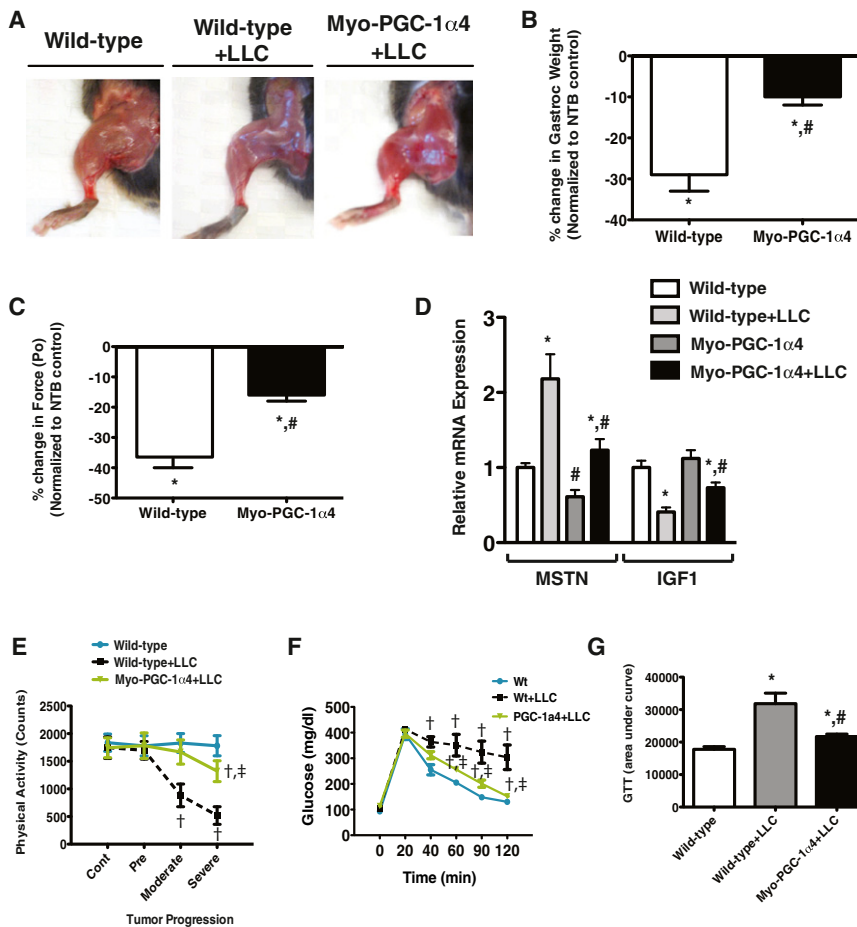


### Figure 7. PGC-1 $\alpha$ 4 Transgenic Mice Show Resistance to Muscle Wasting during Experimental Cancer Cachexia

(A) Representative images of hindlimb muscles from wild-type and tumor-bearing (+LLC) wild-type or Myo-PGC-1 $\alpha$ 4 mice.

(B) Gastrocnemius muscle mass in wild-type and Myo-PGC-1 $\alpha$ 4 tumor-bearing mice normalized to their own genotype non-tumor-bearing control.

(C) Muscle force production in wild-type and Myo-PGC-1 $\alpha$ 4 tumor-bearing mice normalized to their own genotype non-tumor-bearing control.

(D) Myostatin and IGF-1 mRNA expression in wild-type and Myo-PGC-1 $\alpha$ 4 with or without LLC tumor.

(E) Physical activity throughout the progression of tumor load.

(F) Glucose tolerance test.

(G) Quantification of glucose clearance. Bars depict mean values, and error bars represent SE. \* $p < 0.05$  between indicated group and its genotype control. # $p < 0.05$  between indicated group and group receiving same treatment across genotypes. \*,# $p < 0.05$  between all groups. † $p < 0.05$  between indicated group and wild-type mice. ‡ $p < 0.05$  between indicated group and wild-type + LLC mice.

See also Figure S7.

mice (Figure 7A). Strikingly, tumor-bearing Myo-PGC-1 $\alpha$ 4 mice lost only 10% of gastrocnemius muscle mass (Figure 7B), compared to wild-type tumor-bearing animals (29%). This was accompanied by improvements in both muscle force production and myofiber cross-sectional area (Figures 7C and S7A). Cancer-induced cachexia has been shown to occur concomitantly with dysregulation of myostatin and IGF1 expression in muscle (Busquets et al., 2012; Fearon et al., 2012; White et al., 2011). Analysis of muscle gene expression in the different groups revealed that cachectic wild-type animals indeed have a 2.2-fold increase in myostatin gene expression, but only a 1.2-fold increase was seen in tumor-bearing Myo-PGC-1 $\alpha$ 4 animals (Figure 7D). Conversely, IGF1 gene expression was 59% lower in cachectic wild-type muscle, whereas the corresponding Myo-PGC-1 $\alpha$ 4 mice showed only a 27% reduction (Figure 7D). SMAD phosphorylation, a marker of myostatin signal transduction, was clearly suppressed in the Myo-PGC-1 $\alpha$ 4 mice (Figure S7B). The expression of other muscle wasting markers such as MuRF1 and atrogin1/MAFbx1 (Figure S7C) was also strongly reduced in cachectic Myo-PGC-1 $\alpha$ 4 mice (2.3- and 1.9-fold, respectively) when compared to wild-type tumor-bearing controls (5.6- and 7.1-fold, respectively). Tumors in both genotypes of mice grew at the same rates (Figure S7D). Wild-type and Myo-PGC-1 $\alpha$ 4 mice were studied throughout

the development of the cachexia phenotype for physical activity, glucose tolerance, and food consumption. No changes in food intake were observed between wild-type and Myo-PGC-1 $\alpha$ 4 mice with or without LLC cell inoculation (Figure S7E). Although physical activity was similar between wild-type and Myo-PGC-1 $\alpha$ 4 mice before the inoculation of the cancer cells (Figure 7E), it declined more strongly with tumor load in wild-type than in Myo-PGC-1 $\alpha$ 4 mice (Figure 7E). Tumor-bearing Myo-PGC-1 $\alpha$ 4 mice displayed improved glucose tolerance compared to cachectic wild-type mice, as shown by their ability to clear a bolus of glucose (Figures 7F and 7G). Thus, transgenic expression of PGC-1 $\alpha$ 4 in muscle dramatically ameliorates cancer-induced cachexia through reduced loss of muscle mass and strength and improved glucose homeostasis during cancer progression.

## DISCUSSION

Exercise is usually considered in two broad categories: endurance training, which involves low-resistance work of longer duration, and resistance training, which requires more powerful movements of shorter duration. Health studies suggest that most humans should participate in both types of exercise, especially in aging populations (Nair, 2005). Molecular mechanisms underlying the different exercise modalities are not well understood, but the importance of maintaining muscle mass and strength as humans age has motivated considerable research into the pathways of muscle growth; these have highlighted the importance of the IGF1 and myostatin systems (Schiaffino

and Mammucari, 2011; Lee, 2004; McPherron et al., 1997). PGC-1 $\alpha$ , now termed PGC-1 $\alpha$ 1, is induced by exercise and regulates many of the effects of endurance training: mitochondrial biogenesis, fiber-type switching, angiogenesis, and resistance to muscle atrophy. However, gain-of-function studies with PGC-1 $\alpha$  have not shown any increase in either muscle mass or strength (Lin et al., 2002; Sandri et al., 2006; Wende et al., 2007). Similarly, other PGC-1 $\alpha$  variants have been shown to specifically affect energy metabolism in BAT and skeletal muscle, but no effects on cell size have been reported (Tadaishi et al., 2011; Yoshioka et al., 2009; Zhang et al., 2009).

Here, we show that the *Pgc-1 $\alpha$*  gene encodes a protein (PGC-1 $\alpha$ 4) that is expressed robustly in muscle and is particularly induced by resistance training. The *Pgc-1 $\alpha$*  gene has been shown to be subject to alternative splicing, but the PGC-1 $\alpha$ 4 isoform is undescribed. It is somewhat similar to the NT-PGC-1 $\alpha$  isoform (Zhang et al., 2009), but PGC-1 $\alpha$ 4 comes from a different gene promoter and has a completely distinct N terminus derived from the upstream exon 1. Our data strongly suggest that the distinct N-terminal sequence of the PGC-1 $\alpha$ 4 is important in allowing this protein to accumulate in skeletal muscle and perhaps in other tissues.

PGC-1 $\alpha$ 4 specifically activates the expression of IGF1 and suppresses myostatin in skeletal muscle. That the net result of PGC-1 $\alpha$ 4 expression in cultured myotubes represents bona fide hypertrophy, as opposed to hyperplasia, can be deduced from the fact that protein content per unit DNA doubles. In a classical cellular system of muscle cell hypertrophy, stimulation with clenbuterol, PGC1 $\alpha$ 4 is required for this increase in myotube size. PGC-1 $\alpha$ 4 also induces muscle fiber hypertrophy in vivo in three independent expression systems used here: transduction with adenoviral vectors, delivery of naked DNA, and transgenic expression with a muscle-selective promoter. All of these systems give very comparable results, with muscle fiber hypertrophy, modulation of myostatin expression, and in some cases, increases in IGF1 expression. Importantly, we see no changes in mitochondrial gene expression, which is a virtual hallmark of PGC-1 $\alpha$ 1 expression in skeletal muscle. This could be partly explained by the fact that PGC-1 $\alpha$ 4 does not robustly coactivate ERRs.

Transgenic mice with an increase in PGC-1 $\alpha$ 4 expression within or close to the physiological range results in a 60% decrease in myostatin mRNA expression. This is comparable to the 50% decrease observed in mice heterozygous for a null mutation in the myostatin gene. Muscle mass changes in myostatin heterozygous mice range from 7% to 35%, depending on the muscle type and study (Gentry et al., 2011; Lee, 2007; Mendias et al., 2006). The changes observed in the Myo-PGC-1 $\alpha$ 4 mouse are comparable to those reported in two of those studies (Gentry et al., 2011; Mendias et al., 2006). Although effects on other molecular systems are entirely plausible, the effect of PGC-1 $\alpha$ 4 on myostatin gene expression is likely to be a major contributor to the phenotype seen in the Myo-PGC-1 $\alpha$ 4 animals.

Importantly, PGC-1 $\alpha$ 4 transgenic mice have an increase in muscle force production proportional to the increase in muscle mass, indicating that forced PGC-1 $\alpha$ 4 expression in muscle results in functional hypertrophy. The increase in muscle mass and strength results in other significant functional conse-

quences, including exercise tolerance and resistance to hindlimb suspension-induced muscle atrophy. The transgenic expression of PGC-1 $\alpha$ 4 also had a strikingly protective effect in the pathogenesis of cancer-induced cachexia. Although tumors grew at an equal rate in mice of both genotypes, tumor-bearing Myo-PGC-1 $\alpha$ 4 mice lose less muscle mass and strength than controls and do not develop the glucose intolerance observed in the cachectic control animals. This protective effect is clearly reflected in the spontaneous physical activity of the tumor-bearing transgenic animals, which approaches that of non-tumor-bearing wild-type controls, even in the most severe phases of tumor development.

Because PGC-1 $\alpha$ 4 contains the complete activation domain also present in PGC-1 $\alpha$ 1, it seems highly likely that PGC-1 $\alpha$ 4 also functions as a coactivator. However, because PGC-1 $\alpha$ 1 does not stimulate IGF1 and myostatin gene expression, PGC-1 $\alpha$ 4 may be interacting with a very different set of DNA-binding proteins. Interestingly, histone deacetylase (HDAC) inhibition can induce muscle hypertrophy (Iezzi et al., 2004) through a mechanism that involves induction of follistatin expression and increased myoblast recruitment and fusion. Follistatin is a negative regulator of myostatin action and therefore acts positively on muscle mass independent of the IGF1 pathway (Iezzi et al., 2004). We have observed a reduction in follistatin mRNA levels upon PGC-1 $\alpha$ 4 expression (Figure 2F), which would suggest that it does not contribute to PGC-1 $\alpha$ 4-induced muscle hypertrophy. In agreement with this result, PGC-1 $\alpha$ 4 can promote myotube hypertrophy without an increase in myoblast fusion (Figure S3A).

Finally, the potential of PGC-1 $\alpha$ 4 in therapeutics seems obvious. Loss of muscle mass and strength in aging, wasting diseases and in certain muscular dystrophies affects both quality of life and longevity. While protein therapeutics for both the IGF1 and the myostatin pathways are being developed, PGC-1 $\alpha$ 4 can, in principle, modulate both of these systems in a highly coordinated way. Because PGC-1 $\alpha$ 4 comes from a distinct promoter with some degree of distinct regulation in vivo, it will be important to find chemical matter that can modulate PGC-1 $\alpha$ 4 gene expression. In addition, PGC-1 $\alpha$ 4 gene expression might be used as a helpful readout for optimizing resistance training that focuses on increasing muscle strength.

## EXPERIMENTAL PROCEDURES

### PGC-1 $\alpha$ Isoform Cloning and Detection

PGC-1 $\alpha$  isoforms were cloned from a mouse soleus cDNA library. Primer sequences used for cloning and for quantitative real-time PCR detection of the different isoforms in mouse and human tissues can be found in [Extended Experimental Procedures](#).

### Cell Culture, Western Blotting, and Immunocytochemistry

Primary satellite cells (myoblasts) were isolated, maintained, and differentiated as described previously (Megeny et al., 1996). To detect all PGC-1 $\alpha$  variants by immunoblotting, anti-PGC-1 $\alpha$  antibodies were obtained from Calbiochem (ST1202). For PGC-1 $\alpha$  isoform immunoprecipitation experiments, antibodies were obtained from Santa Cruz Biotechnologies (sc-13067).

### Adenovirus-Mediated Expression

Adenovirus expressing the different mouse PGC1 $\alpha$  isoforms or GFP was generated by using the pAdTrack/pAdEasy system (Stratagene). For cell

culture experiments, differentiated myotubes were transduced with an adenovirus at an MOI of 100 overnight. For intramuscular delivery of adenovirus, PGC1 $\alpha$ 4 or GFP viral stock (10  $\mu$ l,  $2 \times 10^{10}$  infectious particles) was injected into the lower limbs of young SCID mice. Each mouse received the control adenovirus in one limb and the PGC-1 $\alpha$ 4 in the contralateral limb. Tissues were harvested 7 days after injection.

### Clenbuterol-Induced Myotube Hypertrophy and PGC-1 $\alpha$ 4

#### Knockdown

Differentiated primary myotubes were treated with 500 nM clenbuterol (Sigma) and PGC-1 $\alpha$ 4 shRNA (ATA AAT GTG CCA TAT CTT CCA) or scrambled shRNA for 48 hr. Cells were then divided in aliquots for genomic DNA and total protein quantification.

#### Chromatin Immunoprecipitation

ChIP was carried out according to a protocol from Upstate Biotechnology. Input DNA and immunoprecipitated DNA were analyzed by quantitative PCR. Primer sequences used to detect each DNA region are available upon request.

#### Electric-Pulse-Mediated Gene Transfer

Electric-pulse-mediated gene transfer was modified from previous studies (Mir et al., 1999). A detailed description can be found in [Extended Experimental Procedures](#).

#### Fiber Type and Cross-Sectional Area Determination

Fiber type determination was done as previously described (Arany et al., 2007). CSA was determined with ImageJ software.

#### Hindlimb Suspension and Reloading

HS was performed as described previously (Hanson et al., 2010). All protocols were approved by the University of Colorado Institutional Animal Care and Use Committee. A detailed description is included in [Extended Experimental Procedures](#).

#### Human Exercise Training

Table S1 provides a complete description of the exercise programs, and a detailed protocol can be found in [Extended Experimental Procedures](#).

#### Generation of Transgenic Mice and Animal Experimentation

Generation of Myo-PGC-1 $\alpha$ 4 mice was done by cloning the PGC-1 $\alpha$ 4 cDNA in front of a MEF2C enhancer/Myogenin promoter DNA sequences (Li et al., 2005), followed by the human growth hormone polyA. Mice were maintained under standard conditions. All experiments and protocols were performed in accordance with the Dana-Farber Cancer Institute or Beth Israel Deaconess Medical Center Animal Facility Institutional Animal Care and Use Committee regulations.

#### Muscle Force Measurements

Maximal muscle force was measured as previously described (Axell et al., 2006) with an isometric transducer (ADI Instruments, Colorado Springs, CO). Specific maximal force was quantified by correcting for muscle mass. A fatigue test was performed following the maximal contractions.

#### Exercise Tolerance Test

Exercise tolerance was performed as previously described (Arany et al., 2007).

#### Cachexia Studies

Wild-type and Myo-PGC-1 $\alpha$ 4 mice were given a subcutaneous injection in the left flank of either  $10^7$  LLC cells in PBS or PBS alone (control). Stages of tumor severity were defined as follows: Pre (before development of tumor), 1–5 days after inoculation; Moderate (moderate tumor size), 10–15 days after inoculation; and Severe (large tumor size), ~23–28 days after inoculation. Mice with tumor development were sacrificed 28 days after injection.

#### Statistical Analysis

All results are expressed as means  $\pm$ SD for cell experiments and  $\pm$ SEM for animal experiments. Two-tailed Student's *t* test was used to determine *p* values. Statistical significance was defined as *p* < 0.05.

### ACCESSION NUMBERS

The GenBank accession numbers for mRNA sequences are JX866946, JX866947, and JX866948. Microarray data are deposited at GEO with the accession number GSE42473.

### SUPPLEMENTAL INFORMATION

Supplemental Information includes Extended Experimental Procedures, seven figures, and one table and can be found with this article online at <http://dx.doi.org/10.1016/j.cell.2012.10.050>.

### ACKNOWLEDGMENTS

We thank Drs. Srikrupa Devarakonda and Sibylle Jäger for valuable discussions. ERR $\alpha$  and ERR $\gamma$  KO myoblasts were a kind gift from Dr. Zhidan Wu (Novartis Institutes for Biomedical Research). The MEF2C/Myogenin promoter cassette was kindly provided by Dr. Eric Olson (University of Texas Southwestern Medical Center). LLC cells were kindly donated by Dr. Jose M. Garcia (Baylor College of Medicine). This project was supported by grants (DK061562) from the NIH and from Novartis to B.M.S. J.L.R. was supported in part by a grant from the Wenner-Gren Foundations, Sweden. This research was supported in part by grants to B.C.H. (NIH, 5K01AR55676-2), N.P.G. (NIH, T32HL07284), J.W. (AHA, 09POST2010078 and 12SDG8070003), B.A.I. (RR024151 and AG09531), Z.Y. (NIH, AR050429), and L.A.L. (NIH, GM29090). B.M.S. is a shareholder and consultant to Ember Therapeutics and has received funding in the form of sponsored research from Novartis, Inc.

Received: February 1, 2012

Revised: June 30, 2012

Accepted: October 26, 2012

Published: December 6, 2012

### REFERENCES

- Adams, G.R. (2002). Invited review: autocrine/paracrine IGF-I and skeletal muscle adaptation. *J. Appl. Physiol.* 93, 1159–1167.
- Arany, Z. (2008). PGC-1 coactivators and skeletal muscle adaptations in health and disease. *Curr. Opin. Genet. Dev.* 18, 426–434.
- Arany, Z., Lebrasseur, N., Morris, C., Smith, E., Yang, W., Ma, Y., Chin, S., and Spiegelman, B.M. (2007). The transcriptional coactivator PGC-1 $\beta$  drives the formation of oxidative type IIX fibers in skeletal muscle. *Cell Metab.* 5, 35–46.
- Axell, A.M., MacLean, H.E., Plant, D.R., Harcourt, L.J., Davis, J.A., Jimenez, M., Handelsman, D.J., Lynch, G.S., and Zajac, J.D. (2006). Continuous testosterone administration prevents skeletal muscle atrophy and enhances resistance to fatigue in orchidectomized male mice. *Am. J. Physiol. Endocrinol. Metab.* 291, E506–E516.
- Bodine, S.C., Latres, E., Baumhueter, S., Lai, V.K., Nunez, L., Clarke, B.A., Poueymirou, W.T., Panaro, F.J., Na, E., Dharmarajan, K., et al. (2001). Identification of ubiquitin ligases required for skeletal muscle atrophy. *Science* 294, 1704–1708.
- Busquets, S., Toledo, M., Orpí, M., Massa, D., Porta, M., Capdevila, E., Padilla, N., Frailis, V., López-Soriano, F.J., Han, H.Q., and Argilés, J.M. (2012). Myostatin blockage using actRIIB antagonism in mice bearing the Lewis lung carcinoma results in the improvement of muscle wasting and physical performance. *J. Cachexia Sarcopenia Muscle* 3, 37–43.
- Chakkalakal, J.V., Nishimune, H., Ruas, J.L., Spiegelman, B.M., and Sanes, J.R. (2010). Retrograde influence of muscle fibers on their innervation revealed by a novel marker for slow motoneurons. *Development* 137, 3489–3499.
- Chinsomboon, J., Ruas, J., Gupta, R.K., Thom, R., Shoag, J., Rowe, G.C., Sawada, N., Raghuram, S., and Arany, Z. (2009). The transcriptional coactivator PGC-1 $\alpha$  mediates exercise-induced angiogenesis in skeletal muscle. *Proc. Natl. Acad. Sci. USA* 106, 21401–21406.

- Choi, C.S., Befroy, D.E., Codella, R., Kim, S., Reznick, R.M., Hwang, Y.J., Liu, Z.X., Lee, H.Y., Distefano, A., Samuel, V.T., et al. (2008). Paradoxical effects of increased expression of PGC-1 $\alpha$  on muscle mitochondrial function and insulin-stimulated muscle glucose metabolism. *Proc. Natl. Acad. Sci. USA* 105, 19926–19931.
- Das, S.K., Eder, S., Schauer, S., Diwok, C., Temmel, H., Guertl, B., Gorkiewicz, G., Tamilarasan, K.P., Kumari, P., Trauner, M., et al. (2011). Adipose triglyceride lipase contributes to cancer-associated cachexia. *Science* 333, 233–238.
- Dinchuk, J.E., Cao, C., Huang, F., Reeves, K.A., Wang, J., Myers, F., Cantor, G.H., Zhou, X., Attar, R.M., Gottardis, M., and Carboni, J.M. (2010). Insulin receptor (IR) pathway hyperactivity in IGF-IR null cells and suppression of downstream growth signaling using the dual IGF-IR/IR inhibitor, BMS-754807. *Endocrinology* 151, 4123–4132.
- Fearon, K.C., Glass, D.J., and Guttridge, D.C. (2012). Cancer cachexia: mediators, signaling, and metabolic pathways. *Cell Metab.* 16, 153–166.
- Florini, J.R. (1987). Hormonal control of muscle growth. *Muscle Nerve* 10, 577–598.
- Gentry, B.A., Ferreira, J.A., Phillips, C.L., and Brown, M. (2011). Hindlimb skeletal muscle function in myostatin-deficient mice. *Muscle Nerve* 43, 49–57.
- Giguère, V. (2008). Transcriptional control of energy homeostasis by the estrogen-related receptors. *Endocr. Rev.* 29, 677–696.
- Gomes, M.D., Lecker, S.H., Jagoe, R.T., Navon, A., and Goldberg, A.L. (2001). Atrogin-1, a muscle-specific F-box protein highly expressed during muscle atrophy. *Proc. Natl. Acad. Sci. USA* 98, 14440–14445.
- Handschin, C., Choi, C.S., Chin, S., Kim, S., Kawamori, D., Kurpad, A.J., Neubauer, N., Hu, J., Mootha, V.K., Kim, Y.B., et al. (2007). Abnormal glucose homeostasis in skeletal muscle-specific PGC-1 $\alpha$  knockout mice reveals skeletal muscle-pancreatic beta cell crosstalk. *J. Clin. Invest.* 117, 3463–3474.
- Hanson, A.M., Stodieck, L.S., Cannon, C.M., Simske, S.J., and Ferguson, V.L. (2010). Seven days of muscle re-loading and voluntary wheel running following hindlimb suspension in mice restores running performance, muscle morphology and metrics of fatigue but not muscle strength. *J. Muscle Res. Cell Motil.* 37, 141–153.
- Heard, E., Rougeulle, C., Arnaud, D., Avner, P., Allis, C.D., and Spector, D.L. (2001). Methylation of histone H3 at Lys-9 is an early mark on the X chromosome during X inactivation. *Cell* 107, 727–738.
- Iezzi, S., Di Padova, M., Serra, C., Caretti, G., Simone, C., Maklan, E., Minetti, G., Zhao, P., Hoffman, E.P., Puri, P.L., and Sartorelli, V. (2004). Deacetylase inhibitors increase muscle cell size by promoting myoblast recruitment and fusion through induction of follistatin. *Dev. Cell* 6, 673–684.
- Lee, S.J. (2004). Regulation of muscle mass by myostatin. *Annu. Rev. Cell Dev. Biol.* 20, 61–86.
- Lee, S.J. (2007). Quadrupling muscle mass in mice by targeting TGF- $\beta$  signaling pathways. *PLoS ONE* 2, e789.
- Li, S., Czubryt, M.P., McAnally, J., Bassel-Duby, R., Richardson, J.A., Wiebel, F.F., Nordheim, A., and Olson, E.N. (2005). Requirement for serum response factor for skeletal muscle growth and maturation revealed by tissue-specific gene deletion in mice. *Proc. Natl. Acad. Sci. USA* 102, 1082–1087.
- Lin, J., Wu, H., Tarr, P.T., Zhang, C.Y., Wu, Z., Boss, O., Michael, L.F., Puigserver, P., Isotani, E., Olson, E.N., et al. (2002). Transcriptional co-activator PGC-1 $\alpha$  drives the formation of slow-twitch muscle fibres. *Nature* 418, 797–801.
- McMillan, D.N., Noble, B.S., and Maltin, C.A. (1992). The effect of the beta-adrenergic agonist clenbuterol on growth and protein metabolism in rat muscle cell cultures. *J. Anim. Sci.* 70, 3014–3023.
- McPherron, A.C., Lawler, A.M., and Lee, S.J. (1997). Regulation of skeletal muscle mass in mice by a new TGF- $\beta$  superfamily member. *Nature* 387, 83–90.
- Megeney, L.A., Perry, R.L., LeCouter, J.E., and Rudnicki, M.A. (1996). bFGF and LIF signaling activates STAT3 in proliferating myoblasts. *Dev. Genet.* 19, 139–145.
- Mendias, C.L., Marcin, J.E., Calderon, D.R., and Faulkner, J.A. (2006). Contractile properties of EDL and soleus muscles of myostatin-deficient mice. *J. Appl. Physiol.* 101, 898–905.
- Mir, L.M., Bureau, M.F., Gehl, J., Rangara, R., Rouy, D., Caillaud, J.M., De-laere, P., Branellec, D., Schwartz, B., and Scherman, D. (1999). High-efficiency gene transfer into skeletal muscle mediated by electric pulses. *Proc. Natl. Acad. Sci. USA* 96, 4262–4267.
- Nair, K.S. (2005). Aging muscle. *Am. J. Clin. Nutr.* 81, 953–963.
- Ogryzko, V.V., Schiltz, R.L., Russanova, V., Howard, B.H., and Nakatani, Y. (1996). The transcriptional coactivators p300 and CBP are histone acetyltransferases. *Cell* 87, 953–959.
- Pende, M., Um, S.H., Mieulet, V., Sticker, M., Goss, V.L., Mestan, J., Mueller, M., Fumagalli, S., Kozma, S.C., and Thomas, G. (2004). S6K1(-)/S6K2(-) mice exhibit perinatal lethality and rapamycin-sensitive 5'-terminal oligopyrimidine mRNA translation and reveal a mitogen-activated protein kinase-dependent S6 kinase pathway. *Mol. Cell. Biol.* 24, 3112–3124.
- Sandri, M., Lin, J., Handschin, C., Yang, W., Arany, Z.P., Lecker, S.H., Goldberg, A.L., and Spiegelman, B.M. (2006). PGC-1 $\alpha$  protects skeletal muscle from atrophy by suppressing FoxO3 action and atrophy-specific gene transcription. *Proc. Natl. Acad. Sci. USA* 103, 16260–16265.
- Schiaffino, S., and Mammucari, C. (2011). Regulation of skeletal muscle growth by the IGF1-Akt/PKB pathway: insights from genetic models. *Skeletal Muscle* 1, 4.
- Short, K.R., Vittone, J.L., Bigelow, M.L., Proctor, D.N., Rizza, R.A., Coenen-Schimke, J.M., and Nair, K.S. (2003). Impact of aerobic exercise training on age-related changes in insulin sensitivity and muscle oxidative capacity. *Diabetes* 52, 1888–1896.
- Tadaishi, M., Miura, S., Kai, Y., Kano, Y., Oishi, Y., and Ezaki, O. (2011). Skeletal muscle-specific expression of PGC-1 $\alpha$ -b, an exercise-responsive isoform, increases exercise capacity and peak oxygen uptake. *PLoS ONE* 6, e28290.
- Wende, A.R., Schaeffer, P.J., Parker, G.J., Zechner, C., Han, D.H., Chen, M.M., Hancock, C.R., Lehman, J.J., Huss, J.M., McClain, D.A., et al. (2007). A role for the transcriptional coactivator PGC-1 $\alpha$  in muscle refueling. *J. Biol. Chem.* 282, 36642–36651.
- Wenz, T., Rossi, S.G., Rotundo, R.L., Spiegelman, B.M., and Moraes, C.T. (2009). Increased muscle PGC-1 $\alpha$  expression protects from sarcopenia and metabolic disease during aging. *Proc. Natl. Acad. Sci. USA* 106, 20405–20410.
- White, J.P., Baynes, J.W., Welle, S.L., Kostek, M.C., Matesic, L.E., Sato, S., and Carson, J.A. (2011). The regulation of skeletal muscle protein turnover during the progression of cancer cachexia in the Apc(Min/+) mouse. *PLoS ONE* 6, e24650.
- Yoshioka, T., Inagaki, K., Noguchi, T., Sakai, M., Ogawa, W., Hosooka, T., Iguuchi, H., Watanabe, E., Matsuki, Y., Hiramatsu, R., and Kasuga, M. (2009). Identification and characterization of an alternative promoter of the human PGC-1 $\alpha$  gene. *Biochem. Biophys. Res. Commun.* 381, 537–543.
- Zhang, Y., Huypens, P., Adamson, A.W., Chang, J.S., Henagan, T.M., Boudreau, A., Lenard, N.R., Burk, D., Klein, J., Perwitz, N., et al. (2009). Alternative mRNA splicing produces a novel biologically active short isoform of PGC-1 $\alpha$ . *J. Biol. Chem.* 284, 32813–32826.